

# Structural, optical and electrical properties of ZnO: B thin films with different thickness for bifacial a-Si:H/c-Si heterojunction solar cells

Dong XU, Sheng YIN (✉), Xiangbin ZENG, Song YANG, Xixing WEN

School of Optical and Electronic Information, Huazhong University of Science and Technology, Wuhan 430074, China

© Higher Education Press and Springer-Verlag Berlin Heidelberg 2016

**Abstract** Textured surface boron-doped zinc oxide (BZO) thin films were fabricated by metal organic chemical vapor deposition as transparent conductive oxide (TCO) for solar cells. The surface microstructure was characterized by X-ray diffraction spectrum and scanning electron microscope. The optical transmittance was shown by optical transmittance microscope and the electrical properties were tested by Hall measurements. The thickness of the BZO film has crucial impact on the surface morphology, optical transmittance, and resistivity. The electrical and optical properties as well as surface microstructure varied inconsistently with the increase of the film thickness. The grain size and the surface roughness increased with the increase of the film thickness. The conductivity increased from  $0.96 \times 10^3$  to  $6.94 \times 10^3$  S/cm while the optical transmittance decreased from above 85% to nearly 80% with the increase of film thickness from 195 to 1021 nm. The BZO films deposited as both front and back transparent electrodes were applied to the bifacial p-type a-Si:H/i-type a-Si:H/n-type c-Si/i-type a-Si:H/n<sup>+</sup>-type a-Si:H heterojunction solar cells to obtain the optimized parameter of thickness. The highest efficiency of all the samples was 17.8% obtained with the BZO film thickness of 829 nm. Meanwhile, the fill factor was 0.676, the open-circuit voltage was 0.63 V and the short-circuit density was 41.79 mA/cm<sup>2</sup>. The properties of the solar cells changing with the thickness were also investigated.

**Keywords** boron-doped zinc oxide (BZO), metal organic chemical vapor deposition (MOCVD), heterojunction solar cell, thickness, textured surface, transparent conductive oxide (TCO)

## 1 Introduction

Due to the high optical transmittance, low resistivity and good stability in plasma environment, boron-doped zinc oxide (BZO) thin films have been proven to be a very promising candidate to replace the indium tin oxide (ITO) as transparent contacts for thin film solar cells [1]. The non-toxicity, low price, abundance of raw material speed up the application of the BZO in photovoltaic devices. Various deposition techniques have been utilized for the fabrication of BZO films such as chemical vapor deposition [2], sputtering [3], sol-gel [4], spray pyrolysis [5] and photo-atomic layer deposition [6], among which the metal organic chemical vapor deposition (MOCVD) and magnetron sputtering are the main techniques for fabricating BZO films. The typical advantages of MOCVD for preparing BZO thin films are relatively low growth temperature and high growth rate. In addition, textured surface BZO can be obtained by MOCVD even without any post-treatment. As we all know, the textured surface of transparent conductive oxide (TCO) could lead to the light trapping effect and enhance the path of the light inside the active layer, and further increase the absorption of light of the cells [7]. Therefore, a thinner active layer is enough to absorb the light resulting from the light trapping effect induced by the textured structure, which will ultimately cut the cost. Furthermore, the phenomenon of light-induced degradation will also be effectively reduced [8].

The path of the light as well as the transmittance determine the probable absorption of light in the active layer, and the photo-generated carriers will be recombined before they reach metal grids of front contacts. Thus the optical and electrical properties of the transparent contact have crucial impact on the performance of the solar cells. In the previous work, we have reported the influence of dopant B and the substrate temperature to the properties of the BZO films [9]. Further investigations are required in

order to clarify the influence of the growth parameters of the BZO films deposited by MOCVD. In this paper, we have studied the influence of thickness on the performance of the bifacial a-Si:H/c-Si heterojunction solar cells.

## 2 Experimental

The ZnO:B films were prepared on the large-scale glasses (230 mm × 230 mm) by MOCVD at low temperature (below 200°C). The precursor gases were diethyl zinc (DEZ), water (H<sub>2</sub>O) vapors carried by argon (Ar) and diborane (B<sub>2</sub>H<sub>6</sub>, H<sub>2</sub>-diluted 1%). The pressure of the reaction chamber was set at 1.0 Torr and the temperature of DEZ were kept at 60°C while the water were kept at 70°C. The substrate temperature was kept at 170°C for all the samples. To obtain the varied thickness of the BZO films, the deposition time were 6, 12, 18, 24 and 30 mins at the B<sub>2</sub>H<sub>6</sub> flow rate of 7 sccm, and obtained the films with the thickness of 195, 383, 607, 829 and 1021 nm, respectively.

The a-Si:H/c-Si heterojunction solar cells were fabricated on n-type (100) c-Si substrate by plasma enhanced chemical vapor deposition (PECVD). To remove the native oxide, the c-Si substrates with the thickness of about 200 μm were dipped in diluted hydrofluoric acid after a standard Radio Corporation of America cleaning. The textured c-Si substrate was obtained by potassium hydroxide (KOH). Then, the intrinsic and doped a-Si:H layers were deposited on the textured n-type c-Si substrate to form p-type a-Si:H/i-type a-Si:H/n-type c-Si/i-type a-Si:H/n<sup>+</sup>-type a-Si:H heterojunction solar cell. The thickness of intrinsic and doped a-Si:H layers were 5 and 10 nm, respectively. Finally, the BZO films were grown on the surface of the heterojunction solar cells as both front and back electrodes by MOCVD. The Ag gridded electrodes were prepared on the solar cells by screen printing method. Other parts of the heterojunction solar cells were fabricated under same condition.

The thickness of films were measured by spectroscopic ellipsometry (SOPRA GES-5E) and X-ray diffraction spectrum were obtained by using a Philips X'Pert Pro (XRD, PANalytical PW 3040/60) at a voltage of 40 kV and a current of 40 mA, with Cu Kα radiation (λ = 1.5406 Å) to investigate the crystallographic structure of BZO films. The surface morphologies of the films were investigated by the scanning electron microscope (SEM). The optical transmittance spectrum of all the samples were performed by 7-SCSPEC solar cell spectral performance testing system, and the range of testing wavelength were from 300 to 1100 nm. The electrical properties of the BZO films were measured by Hall measurement after Al electrodes were deposited on the films. *I-V* characteristic of the bifacial a-Si/c-Si heterojunction solar cell was obtained by Newport solar cell *I-V* testing system (PVIV-94023A).

## 3 Discussion

### 3.1 Structure

Figure 1 shows the XRD patterns of BZO films with thickness from 195 to 1021 nm. The XRD patterns of the BZO films consisted of four diffraction peaks, which are (100), (002), (101) and (110) crystal planes. When the thickness of the film was below 195 nm, all of the diffraction peaks were very weak, which can be attributed to the lateral growth of the thin film in the early age of deposition. The crystal orientation was not clear with no dominate peak appeared. With the increase of film thickness, the (100) and (110) diffraction peaks enhanced due to the increase of crystalline. The intensity of the (110) peak enhanced much obviously than the (100) peak, which revealed that the films had preferred orientation of c-axis parallel to the substrate.

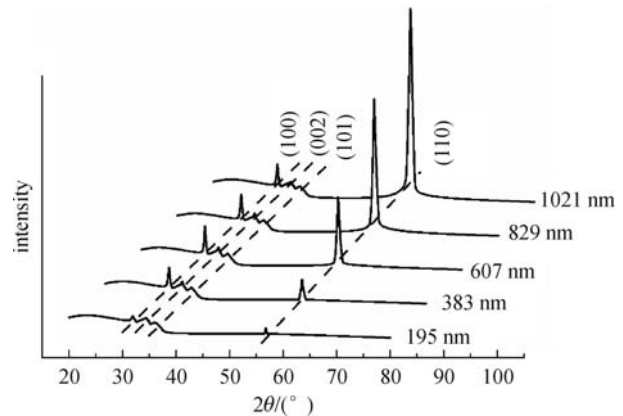


Fig. 1 XRD patterns of BZO films with different thickness

The diffraction angle  $2\theta$  and the full width at half maximum (FWHM) with different thickness are given in Table 1. The lattice constant  $c$  can be calculated by Eqs. (1)–(2):

$$d_{hkl} = \frac{n\lambda}{2\sin\theta}, \quad (1)$$

$$d_{hkl} = \left( \frac{4}{3} \frac{h^2 + hk + k^2}{a^2} + \frac{l^2}{c^2} \right)^{-1/2}, \quad (2)$$

where  $\theta$  is diffraction angle,  $\lambda$  is wavelength of X-ray,  $(hkl)$  is Miller indices of the planes,  $d_{hkl}$  is the interplanar spacing,  $a$  and  $c$  are the lattice constant. Table 1 shows that with the increase of thickness, the diffraction angle increased, so we can deduce from the above equations that with the increase of thickness, the interplanar spacing  $d_{hkl}$  and the lattice constant  $c$  decreased. The crystal size of BZO films can be deduced by the well-known Debye-Scherrer formula:

**Table 1** Variation of the Bragg angle  $2\theta$ , FWHM and crystal size with thickness

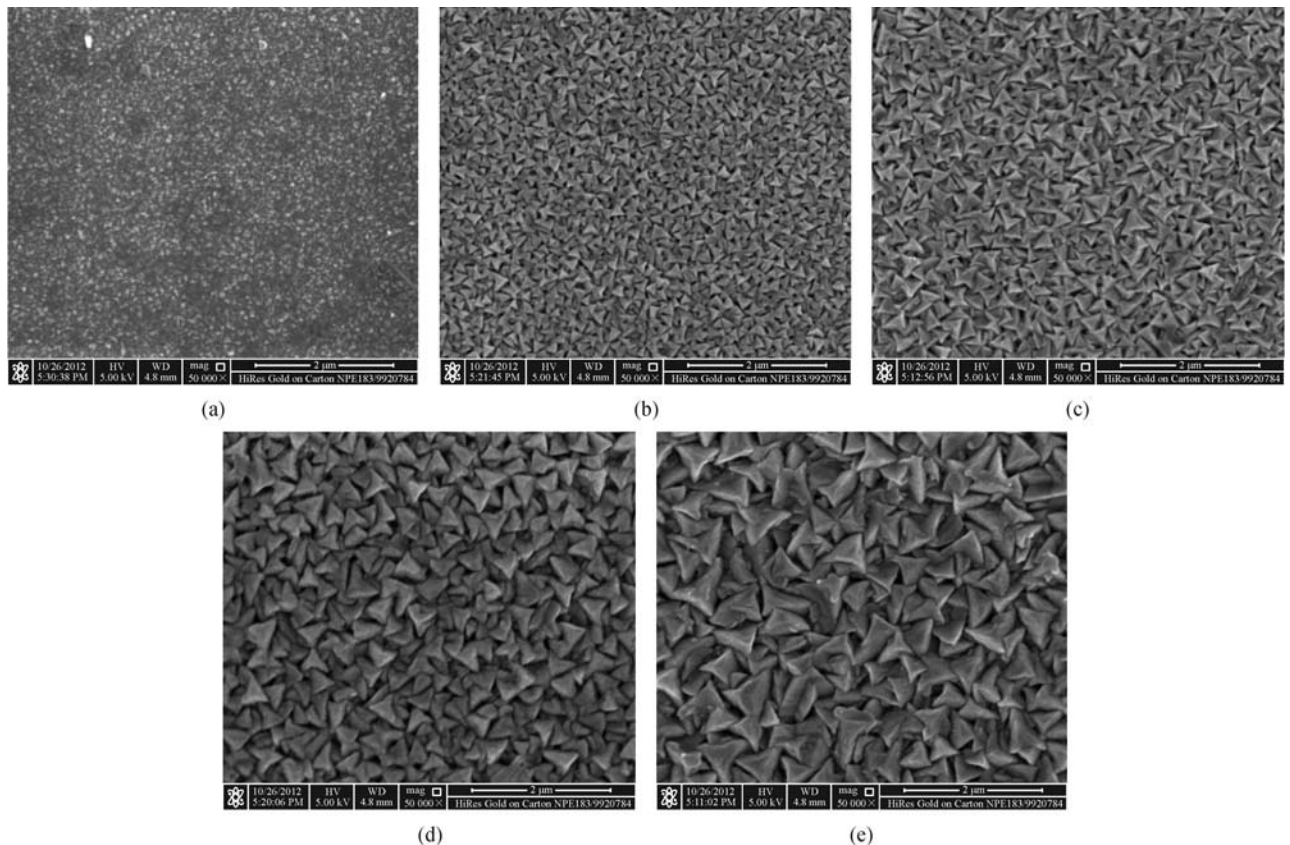
deposition time/mins	thickness/nm	$2\theta/(^\circ)$	FWHM/ $(^\circ)$	$G$ /nm
6	195	56.73	0.44	20.52
12	383	56.80	0.38	23.77
18	607	56.83	0.31	29.13
24	829	56.85	0.26	34.74
30	1021	56.87	0.19	47.54

$$G = \frac{0.9\lambda}{\beta \cos\theta}, \quad (3)$$

where  $G$  is the crystal size,  $\lambda$  is wavelength of X-ray,  $\beta$  is FWHM,  $\theta$  is the half diffraction angle of the centroid of the peak. As shown in Table 1, the FWHM decreased with the increase of thickness. According to the Debye-Scherrer formula, with the increase of thickness, the crystal size  $G$  increased. The above results demonstrated that the thickness plays an important role in the crystalline and the lattice structure of the BZO films.

The SEM micrographs of ZnO:B with different thickness are shown in Fig. 2. The grain size of the BZO films were evaluated from the SEM micrographs by detecting the borders of the grains observable on the surface. The mean projected area of the grains was deduced and the

square root of this value was taken as dimensional parameter for the grain size [10]. The grain was in small size and the surface was relatively flat due to the lateral growth when the film thickness was 195 nm. With the thickness increased to 383 nm, the pyramidal-like surface appeared due to the film grown with the preferred orientation of c-axis parallel to the substrate, which has been discussed from the result of XRD patterns. The grain size was about 80 nm when the film thickness was 383 nm. With the increase of BZO film thickness, the small grains disappeared and the grains accumulated and became larger as well as uniform. When the film thickness was about 1021 nm, the film shown large pyramidal-like grains emerging out of the surface and the grain size was about 280 nm. The rough surface constituted of large pyramidal grains could enhance the light trapping effect, which

**Fig. 2** Surface morphology of the BZO film with the thickness of (a) 195 nm, (b) 383 nm, (c) 607 nm, (d) 829 nm, (e) 1021 nm

increased the path of the light inside the solar cell [7]. Thus, the increase in thickness could improve the light trapping structure for the thin film solar cells.

The difference between the values of crystal size measured by XRD and the values of grain size evaluated from SEM image can be explained as following: the  $G$  calculated with the Scherrer equation is related to crystallographically coherent crystalline unit that diffracts the X-ray and is the average value along the film thickness, while the grain size is evaluated from the SEM images, at the film surface as distance between two visible grain boundaries [10]. Both the grain size and the crystal size showed the same changing trend with the increase of thickness.

### 3.2 Electrical properties

Figure 3(a) shows that the carrier concentration first increased and then kept almost a constant. The carrier concentration was at a relatively low level of  $6.7 \times 10^{19} \text{ cm}^{-3}$  at the thickness of 195 nm. It can be understood as follows: First, the BZO film with thickness of 195 nm had low crystal quality and high defect density, which could trap the free carriers; Second, when a semiconductor is abruptly terminated at the surface, the disruption of potential function would create discrete energy states within the band gap which were called surface states and could trap free carriers [11]. In addition, when the BZO films was exposed to air, the chemisorption of oxygen have more significant affection on the carrier concentration of the thinner BZO films. The chemisorbed oxygen atoms could annihilate the shallow donor energy levels, which come from the oxygen vacancies and lead to the decrease of carrier concentration in thinner films. The carrier density increased with the thickness when it was below 600 nm, and then approached to almost a constant. This phenom-

enon can be attributed to the increase of crystallinity and stability of the BZO films. Figure 3(b) shows that the mobility increased monotonically with the increase of thickness. It can be attributed to two main reasons: 1) The increase of grain size led to the decrease of grain boundary as well as grain boundary scattering; 2) The increase of crystallinity led to the decrease of defect density, which further led to the increase of carrier mobility. As all knows that the resistivity is determined by both carrier concentration  $n$  and mobility  $\mu$ , which can be expressed as  $\rho = 1/(nq\mu)$ . The variation of both  $n$  and  $\mu$  resulted in the change of resistivity. It can be seen from Fig. 3(c) that the resistivity  $\rho$  of BZO films decreased monotonically with the increase of thickness. The minimum resistivity was  $1.33 \times 10^{-4} \Omega \cdot \text{cm}$  at thickness of 1021 nm. Meanwhile, the mobility and carrier concentration of the BZO film were  $25.03 \text{ cm}^2/\text{Vs}$  and  $1.73 \times 10^{20} \text{ cm}^{-3}$ , respectively. Furthermore, a favored low value is the sheet resistance  $R_{\text{sh}}$ , which could be achieved with the increase of thickness  $d$  ( $R_{\text{sh}} = \rho/d$ ).

### 3.3 Optical properties

The transmittance spectrum of the BZO films with various thickness is given in Fig. 4. The film with the thickness of 195 nm had an average transmittance over 85% in the range of visible and infrared light. The average transmittance decreased to about 80% with the thickness increase to 1021 nm due to the thickness effect. Besides, the transmittance also decreased with the wavelength, especially in the long wavelength above 800 nm due to the free carrier absorption (FCA) effect according to Drude theory [12]. The FCA can be described by equation:

$$A = \frac{\lambda^2 e^3 n d}{4\pi^2 \epsilon_0 c^3 N m^{*2} \mu}, \quad (4)$$

where  $A$  is the absorbance index,  $\lambda$  is the wavelength of the incident light,  $e$  is the electron charge,  $n$  is carrier

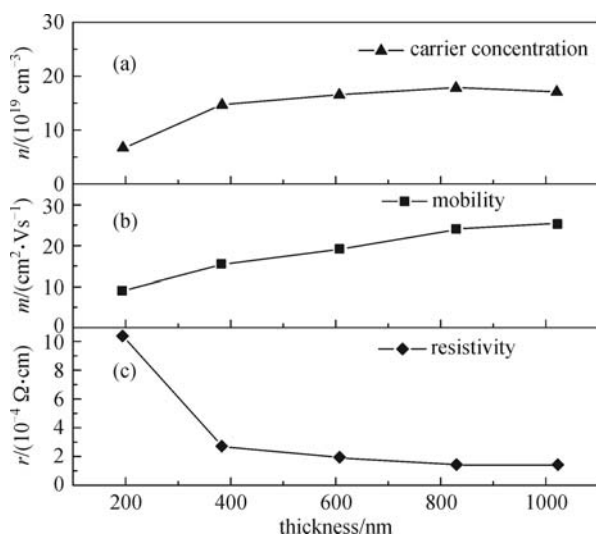


**Fig. 3** Plot of (a) carrier concentration, (b) Hall mobility, and (c) resistivity of the BZO films versus the film thickness

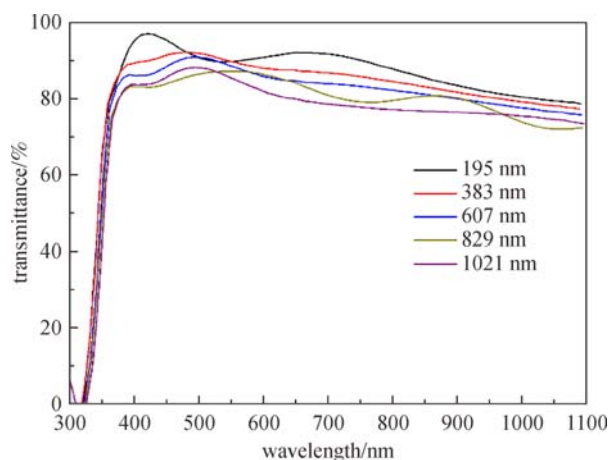


**Fig. 4** Optical transmittance of BZO films with different thickness

concentration,  $d$  is film thickness,  $\varepsilon_0$  is the permittivity of free space,  $c$  is the light velocity,  $N$  is refraction index of the film material,  $m^*$  is effective mass of an electron and  $\mu$  is mobility. Though the increase in thickness could increase the mobility  $\mu$ , the excessive thick BZO films or high carrier concentration could lead to high light absorption in nearinfrared (NIR) range. Therefore the slightly doped ZnO films with proper thickness could suppress the FCA effect in NIR range. In addition, the absorption edge of the BZO films shifted toward long wavelength in general with the increase of thickness which has also been observed by Faÿ as well [13]. It might be the reason that the optical band gap of BZO films was changed. As BZO is direct band gap material, the optical band gap can be deduced from the plot of  $(\alpha h\nu)^2$  versus photo energy  $h\nu$ , where  $\alpha$  is the optical absorption coefficient,  $h$  is Planck constant, and  $\nu$  is the frequency of the incident light. The  $\alpha$  can be obtained by  $d^{-1} \cdot \ln(1/T)$ , where  $d$  is the thickness of BZO film, and  $T$  is the transmittance. Figure 5 gives the Tauc plots of BZO films with various thickness. With the increase of film thickness, the optical band gap of BZO films first increased and then decreased. It could be explained by the follow: According to Burstein-Moss effect, the increase of optical bandgap ( $\Delta E_g$ ) of BZO relative to un-doped ZnO can be given by [14]

$$\Delta E_g = \frac{h^2}{8m^*} \left( \frac{3N_e}{\pi} \right)^{2/3}. \quad (5)$$

$N_e$  is the carrier concentration, and  $m^*$  is the reduced effective mass. Thus when the film was thin, the significant increase of carrier concentration can be the reason of the increase in optical band gap according Burstein-Moss effect [15]. However with the thickness increase further, the optical bandgap decreased and departure from the changing trend of carrier concentration. The decrease in optical bandgap can be explained by the decrease of lattice constant, which has been discussed from the result of XRD

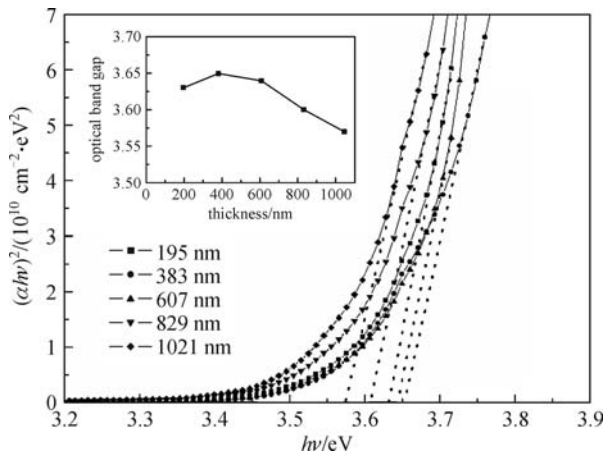


Fig. 5 Tauc plots with different thickness

patterns [16]. The decrease of the lattice constant led to the increase of the overlap of electron orbital and broadened both the conductive band and valence band. Therefore, the optical bandgap become narrow. The determined optical band gaps of BZO films with film thickness of 195, 383, 607, 829 and 1021 nm were 3.63, 3.65, 3.64, 3.6 and 3.57 eV, respectively. As we know, the wider optical bandgap of BZO films which could reduce optical losses and raised the optical utilization efficiency of solar cells were more suitable for electrodes of solar cells. Thus, with the increase of thickness, optical transmittance and absorption edge as well as bandgap deteriorated in general.

### 3.4 Solar cells

To investigate the influence of the optical and electrical properties of BZO films to the solar cells, the BZO films with different thickness were applied to the bifacial p-type-a-Si:H/i-type-a-Si:H/n-type c-Si/i-type a-Si:H/n<sup>+</sup>-type a-Si:H heterojunction solar cells. Figure 6(a) shows the schematic diagram of the bifacial heterojunction solar cells. Figure 6(b) shows the  $I-V$  parameters of solar cells with different thickness of BZO films. The open circuit voltage ( $V_{oc}$ ) first increased from 0.611 to 0.631 V and then decreased slightly to 0.622 V with the increase of thickness. This can be explained by the follows: when the film was thin, the transmittance was relatively high and the major fact that influence the optical properties was the light scattering capability. The increase of thickness could have an obvious enhancement of surface roughness which improved the light scattering capability and improved the  $V_{oc}$ . With the thickness increased further, the optical transmittance of front electrode decreased which reduced the intensity of light in the active layer, and thus led to the decrease of  $V_{oc}$ . The improvement of fill fact ( $FF$ ) from 64.9% to 67.6% could be attributed to the improvement of electrical properties of the ZnO:B electrodes. The short-circuit density ( $J_{sc}$ ) increased from 40.26 to 41.79 mA/cm<sup>2</sup> with the thickness increase from 195 to 829 nm resulting from both the decrease of sheet resistance and the increase of the  $V_{oc}$ . As the thickness increased to 1021 nm, the  $J_{sc}$  decreased to 41.67 mA/cm<sup>2</sup> due to the decrease of the  $V_{oc}$ . The efficiency of the solar cells increased from 16% to 17.8% with the thickness of ZnO:B electrodes increased from 195 to 829 nm and then decrease to 17.5%. Therefore, the thickness of the BZO films has great impact on the performance of solar cells.

## 4 Conclusions

In this paper, we have studied the structure, electrical and optical properties of BZO thin films varied with film thickness. With the increase of BZO film thickness, the surface roughness increased, which enhance the light trapping effect. The resistivity and sheet resistance

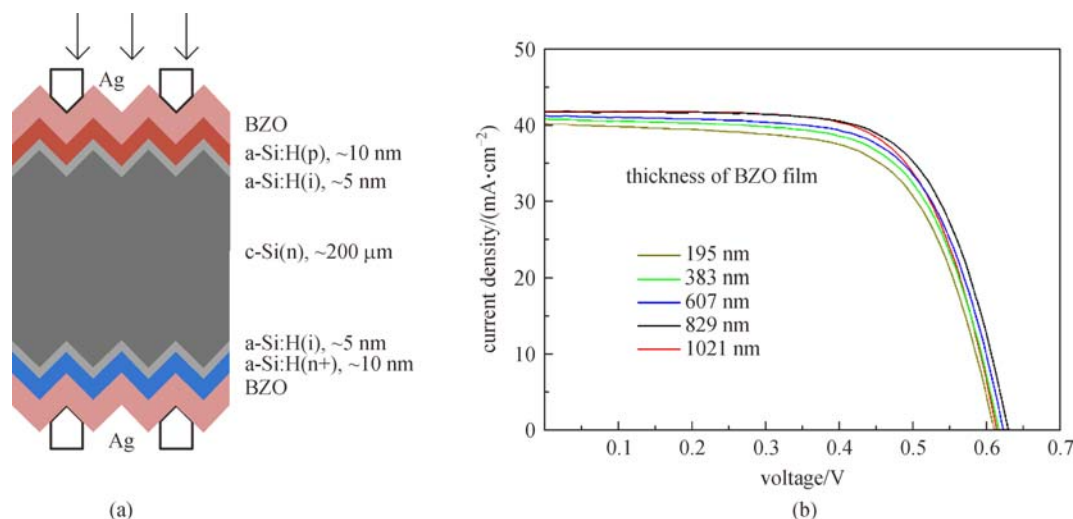


**Fig. 6** (a) Schematic diagram of the bifacial heterojunction solar cells; (b) current density–voltage ( $I$ – $V$ ) curves of the bifacial a-Si:H/c-Si heterojunction solar cells applied with the ZnO:B films of 195–1021 nm as electrodes

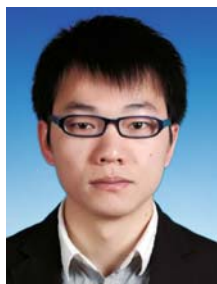
decreased monotonically with the increase of thickness while the optical properties deteriorated, which the transmittance decreased due to the thickness effect and free carrier absorption in NIR. The change of optical bandgap led to the red shift of the absorption edge which also deteriorated the optical properties. Finally, we applied the BZO films to the bifacial a-Si:H/c-Si heterojunction solar cells to get the optimized solar cell, the efficiency of solar cells increased from 16% at the film thickness of 195 nm to the 17.8% of 829 nm and then decreased to 17.5% with the thickness increased further to 1021 nm. The open circuit  $V_{oc}$  was influenced by the optical properties of the BZO films while the short-circuit density  $J_{sc}$  was influenced by both the electrical and optical properties of the BZO films.

**Acknowledgements** This work was supported by the National Natural Science Foundation of China (Grant No. 51472096) and the Supporting Technology Project of Education of China (No. 62501040202). The authors would like to thank all members of the thin film group at the Photonic and Information System Integration Institute for their support of this work and helpful discussion. The authors also thank Analytical and Testing Center of Huazhong University of Science & Technology for SEM measurement and Optoelectronic Micro/nano Fabrication Faculty of Wuhan National Laboratory for XRD and optical measurements and analysis of samples for their valuable suggestions and help for the samples characterizations

## References

- Wenas W W, Yamada A, Takahashi K, Yoshino M, Konagai M. Electrical and optical properties of boron-doped ZnO thin films for solar cells grown by metalorganic chemical vapor deposition. *Journal of Applied Physics*, 1991, 70(11): 7119–7123
- Choi I. Properties of boron-doped ZnO thin films grown by using MOCVD. *Journal of the Korean Physical Society*, 2013, 63(10): 1997–2001
- Gao L, Zhang Y, Zhang J, Xu K. Boron doped ZnO thin films fabricated by RF-magnetron sputtering. *Applied Surface Science*, 2011, 257(7): 2498–2502
- Jana S, Vuk A S, Mallick A, Orel B, Biswas P K. Effect of boron doping on optical properties of sol-gel based nanostructured zinc oxide films on glass. *Materials Research Bulletin*, 2011, 46(12): 2392–2397
- Pawar B N, Jadkar S R, Takwale M G. Deposition and characterization of transparent and conductive sprayed ZnO:B thin films. *Journal of Physics and Chemistry of Solids*, 2005, 66(10): 1779–1782
- Yamamoto Y, Saito K, Takahashi K, Konagai M. Preparation of boron-doped ZnO thin films by photo-atomic layer deposition. *Solar Energy Materials and Solar Cells*, 2001, 65(1-4): 125–132
- Müller J, Rech B, Springer J, Vanecek M. TCO and light trapping in silicon thin film solar cells. *Solar Energy*, 2004, 77(6): 917–930
- Yin J, Zhu H, Wang Y, Wang Z, Gao J, Mai Y, Ma Y, Wan M, Huang Y. A study of ZnO:B films for thin film silicon solar cells. *Applied Surface Science*, 2012, 259:758–763
- Zeng X, Wen X, Sun X, Liao W, Wen Y. Boron-doped zinc oxide thin films grown by metal organic chemical vapor deposition for bifacial a-Si:H/c-Si heterojunction solar cells. *Thin Solid Films*, 2016, 605(30): 257–262
- Addonizio M L, Diletto C. Doping influence on intrinsic stress and carrier mobility of LP-MOCVD-deposited ZnO:B thin films. *Solar Energy Materials and Solar Cells*, 2008, 92(11): 1488–1494
- Dong B, Fang G, Wang J, Guan W, Zhao X. Effect of thickness on structural, electrical, and optical properties of ZnO: Al films deposited by pulsed laser deposition. *Journal of Applied Physics*, 2007, 101(3): 033713-1–033713-7
- Exarhos G J, Zhou X D. Discovery-based design of transparent conducting oxide films. *Thin Solid Films*, 2007, 515(18): 7025–7052
- Fay S. *Science of Microtechnique*, Institute of Production and

- Robotic, école Polytechnique Fédérale de Lausanne, Lausanne, 2003
14. Kumar V, Singh R G, Purohit L P, Mehra R M. Structural, transport and optical properties of boron-doped zinc oxide nanocrystalline. *Journal of Materials Science and Technology*, 2011, 27(6): 481–488
  15. Huang Q, Wang Y, Wang S, Zhang D, Zhao Y, Zhang X. Transparent conductive ZnO:B films deposited by magnetron sputtering. *Thin Solid Films*, 2012, 520(18): 5960–5964
  16. Ton-That C, Foley M, Phillips M R, Tsuzuki T, Smith Z. Correlation between the structural and optical properties of Mn-doped ZnO nanoparticles. *Journal of Alloys and Compounds*, 2012, 522: 114–117



**Dong Xu**, student, Huazhong University of Science and Technology. He studied in Huazhong University of Science and Technology, and received the B.S. degree in electronic science and technology, then studied in Huazhong University of Science and Technology for the M.Eng. degree in microelectronic and solid state electronic. His research interests focus on photovoltaic materials and thin film transistors.



**Sheng Yin**, associate professor, Huazhong University of Science and Technology. He studied in Huazhong University of Science and Technology, and received the B.S. degree in semiconductor physics and devices, the M.Eng. degree in electronic science and technology and the Ph.D. degree in microelectronics and solid state electronics. His research interests focus on at panel displays including a-Si thin film transistors, LTPS thin film transistors, amorphous oxide semiconductor thin film transistors, AM-LCDs and AM-OLEDs.



**Xiangbin Zeng**, professor, Huazhong University of Science and Technology. He studied in Xi'an JiaoTong University, and received the B.S. degree in semiconductor physics and devices, then studied in Huazhong University of Science and Technology, and received the M.Eng. degree in electronic materials and devices, and received the Ph.D. degree in microelectronics and solid state electronics in the same university. From 1998 to 1999, as a visiting scholar, he worked at the Hong Kong University of Science and Technology, Hong Kong, China. From 2001 to 2003, as a Research Fellow, he worked at Nanyang Technological University, Singapore. His research interests focus on ZnO thin film, AZO thin film, BZO thin film, Si nanometer, Si quantum dot and solar cells including c-Si, a-Si thin film, a-Si tandem,  $\mu$ -Si thin film, Si quantum dot solar cell and a-Si/c-Si heterojunction solar cells.



**Song Yang**, student, Huazhong University of Science and Technology. He studied in Wenhua University, and received the B.S. degree in electronic science and technology, then studied in Huazhong University of Science and Technology for the M.Eng. degree in microelectronic and solid state electronic. His research interests focus on integrated circuit design.



**Xixing Wen**, student, Huazhong University of Science and Technology. He studied in Shandong Normal University, and received the B.S. degree in applied physics. Then he studied in Huazhong University of Science and Technology for a Ph.D. degree in microelectronic and solid state electronic. His research interests focus on photovoltaic materials and devices.